Physica A 622 (2023) 128802

Contents lists available at ScienceDirect

Physica A

journal homepage: www.elsevier.com/locate/physa

Statistical study of the EEG in motor tasks (real and imaginary)

F.M. Oliveira Filho [a,b], F.F. Ribeiro [a,e], J.A. Leyva Cruz [c], A.P. Nunes de Castro [d], G.F. Zebende [c,*]

[a] Earth Sciences and Environment Modeling Program, State University of Feira de Santana, Bahia, Brazil
[b] SENAI CIMATEC University Center, Salvador, Bahia, Brazil
[c] State University of Feira de Santana, Bahia, Brazil
[d] Jorge Amado University Center, Salvador, Bahia, Brazil
[e] Federal University of Bahia, Salvador, Bahia, Brazil

ARTICLE INFO

Article history:
Received 12 February 2023
Received in revised form 11 April 2023
Available online 5 May 2023

Keywords:
DFA
DCCA cross-correlation coefficient
EEG
Motor/imaginary human tasks

ABSTRACT

EEG is one of the techniques more used to assess the extent of damage from these deficiencies and even to find solutions such as rehabilitation or limb replacement using a bionic prosthesis, through brain-computer interface. That is why it is of vital importance that we understand the functioning of the primary motor cortex of the brain in the control of real/imaginary tasks. From *Physionet* database, with two-minute EEG recordings in three different experiments (real/imaginary), we applied DFA and DCCA methods to find auto-correlations and cross-correlations. DFA method was capable of quantitatively describing similarities when the brain performs the same motor task, and show there are three time-scales. After, in order to compare the fluctuation amplitude of an EEG signal in relation to the other channels and measure these cross-correlations, we applied $\Delta \log F_{DFA}$ function and ρ_{DCCA} coefficient. Thus, choosing the F_3 channel (front) as the reference, we identified generally that: $\Delta \log F_{DFA}[F_3 : xx] \geq 0$ and $\rho_{DCCA} > 0$. The channels: C_z, F_6, T_9, and T_{10}, are those that have a higher level of DCCA cross-correlation, if compared to the channel F_3. The time scale **II**, with $16 < n \leq 723$, is the one with ρ_{DCCA} maximum. Finally, the statistic applied in this paper, based on the DFA-method, proved to be an excellent candidate for studies of motor functions in the brain computer interface area.

1. Introdution

In medicine one of the most challenging problems nowadays is to decipher how the brain functioning, especially in clinically states, as a physical and/or motor impairment. It could allow us to distinguish between realized and imagined activities in the cerebrum. The human brain spontaneously generates neural bio-electric oscillations [1] with a spread range of variability in frequency, amplitude, the scale of duration, and coherence to permit connectivity of different areas involved mainly, in the higher cortical functions (HCF). The HCF is referring to all cognitive mental activity, for example, thinking, remembering, reasoning, and also complex functions, such as speaking and carrying out a premeditated movement.

Two standard techniques that are essential to study these functions, mainly due to their high temporal resolutions (in order of milliseconds), are the Electroencephalography, that use the electroencephalograms (EEG) [2] signals and the

* Corresponding author.
E-mail addresses: florenciofh@yahoo.com.br (F.M.O. Filho), gfzebende@uefs.br (G.F. Zebende).

https://doi.org/10.1016/j.physa.2023.128802
0378-4371/

Magnetoencephalography that makes use of the so-called magnetoencephalograms (MEG) [3]. The EEG are the temporal series of the bio-electrical voltage signals, measurement on the scalp by electrodes [4]. While the MEGs, are temporal series of the bio-magnetic fields signals, measurement on the scalp using ultra-sensitive magnetometers [5]. Both are signals produced when brain cells or neurons are synchronously activated by external or internal stimuli.

The EEG and the MEG in addition to being considered electrophysiological techniques, it is also seen as neuroimaging techniques, i.e., the reconstruction of electric and magnetic sources inner the cerebral cortex, from the measured on scalp the bio-electromagnetic fields [3,6]. The information that digital EEGs processing reveals in the spectral domain has been used for decades to diagnose several neurological pathologies, such as, in the study of the pain process in humans using evoked potentials [7]; and the diagnosis of epilepsy and autism disorders [8]. The use of a multi-modal approach using the single-photon emission computed tomography (SPECT) and quantitative EEG, have useful to diagnostics of dementia disease [9], and for the location of the epileptogenic zone in pharmacoresistant non-lesional Epilepsy [10]. In other study an integrating approach using EEG, transcranial magnetic stimulation (TMS), and magnetic resonance image (MRI) shown that is a possible way to investigate effective brain connectivity [11]. Also, EEG has been extensively used in the investigations of brain dynamics in pathological states and during cognitive or behavior tasks. Lots of measures have been used to analysis the features of muti-channel EEG signals, such as synchronization, coherence, and functional networks, see [12–15]. Normally, the EEG digital processing, for medical diagnosis purpose using spectral methods, such as Fast Fourier Transform (FFT), Discrete Wavelet Transform (DWT), among other [16–18].

The brain is considered a complex and non-linear dynamic system, and the EEG signals are classified as non-stationary with several fractal characteristics. Therefore, the statistical algorithms applied to stationary signals are not appropriated to the processing of these bio-electric signals. Actually, the bio-signal processing state of art have shown an increase of Detrended Fluctuation Analysis (DFA) based methods to study different human physiological process. For example, [1] reported presence of long-range correlations and power-law scaling behavior within the 10 to 20 Hz band (alpha and beta bands) from MEG/EEG data recorded from 10 subjects with eyes open and closed conditions, for a duration of 20 minutes. The power-law behavior was evident in the time-range of 5–300 seconds and the DFA scaling exponent in both the eyes close and open conditions were 0.68 and 0.70, significantly higher than that reference data, which was 0.5. Applying the DFA method on EEG, was demonstrate long-range temporal correlations with an attenuation of the value of α_{DFA} exponent or lower similarity, in the case of Alzheimer's disease (AD) [19] and schizophrenia [20] diseases. In the case of AD, it was shown that the α_{DFA} exponent was lower in AD patients compared to controls in the alpha band. While in the case of schizophrenia, the α_{DFA} exponent was lower in patients in both alpha and beta bands compared to the healthy controls. The reduction of the α_{DFA} exponent value can be interpreted as a difficulty for patients to remember the past. The value of α_{DFA} could also potentially used as a bio-marker for neurological disorders like AD and schizophrenia, in future clinical studies.

A study demonstrated that the generalized Hurst exponent estimates differentiate EEG signals of healthy and epileptic patients [21]. In another paper, [22] was applied the DFA method to analyze serial changes in heart rhythm complexity from the acute to chronic phase on patients who suffered an acute myocardial infarction (MI), using electrocardiograms (EEGs). The EEGs were measurement on 27 patients with MI with elevation of ST-segment and 42 control subjects. The DFA α_{DFA} exponent had a significantly lower value in the acute stage (within 72 hours) and also, at 3 months and 12 months after MI, in comparison with control. In a newly published paper [23], was demonstrated that the DFA method can be used as a data processing algorithm in brain-computer interfaces, to detected real and imaginary arm movements, in most EEG- channels.

Our group reported in [24,25] a new perspective for application of DFA method, with the root mean square of the fluctuation difference function, $\Delta \log F_{DFA}$, to study the motor real and imaginary human activity using 64-channel EEGs, and also, to the analysis of the EEG during the reading task [26]. In these papers were verified that the amplitude of the F_{DFA} rms function is greater for the frontal channels than for the parietal, and the auto-correlation exponent, α_{DFA}, revealed self-affinity at a specific time scale. The detrended cross-correlation coefficient method, ρ_{DCCA} [27], was applied to analyze EEG signals from AD patients [28]. The ρ_{DCCA} presented to be lower in AD patients when compared with the control group, indicating an alteration of both synchronization and oscillation in EEGs of these patients. An attenuation of synchronization in the whole cerebrum and a bigger scale corresponding to maximum correlation was showed in AD patients.

In this paper, we analyze the brain activity in 11 subjects, in three different experiments, using DFA method, $\Delta \log F_{DFA}$ function, and the cross-correlation coefficient ρ_{DCCA}. The main idea was to analyze the previous methods, at eight EEG channels, between different areas of the brain, described below: Frontal $\mathbf{F}_3$, $\mathbf{F}_6$; Temporal $\mathbf{C}_z$, $\mathbf{T}_9$, $\mathbf{T}_{10}$; Parietal $\mathbf{P}_3$, $\mathbf{P}_6$ and Occipital $\mathbf{I}_z$ (see Fig. 1 for more details). These electrodes were chosen in this configuration because this symmetry covers the entire scalp, see [24,26]. The Fig. 1 shows the schematic diagram of the arrangement of the 64 electrode locations on the scalp, where the EEGs were measured, in accordance with the International 10–10 system. In this way we can investigate EEGs from different channels and quantify how two areas are associated to the same scale, for a response to a motor stimuli action.

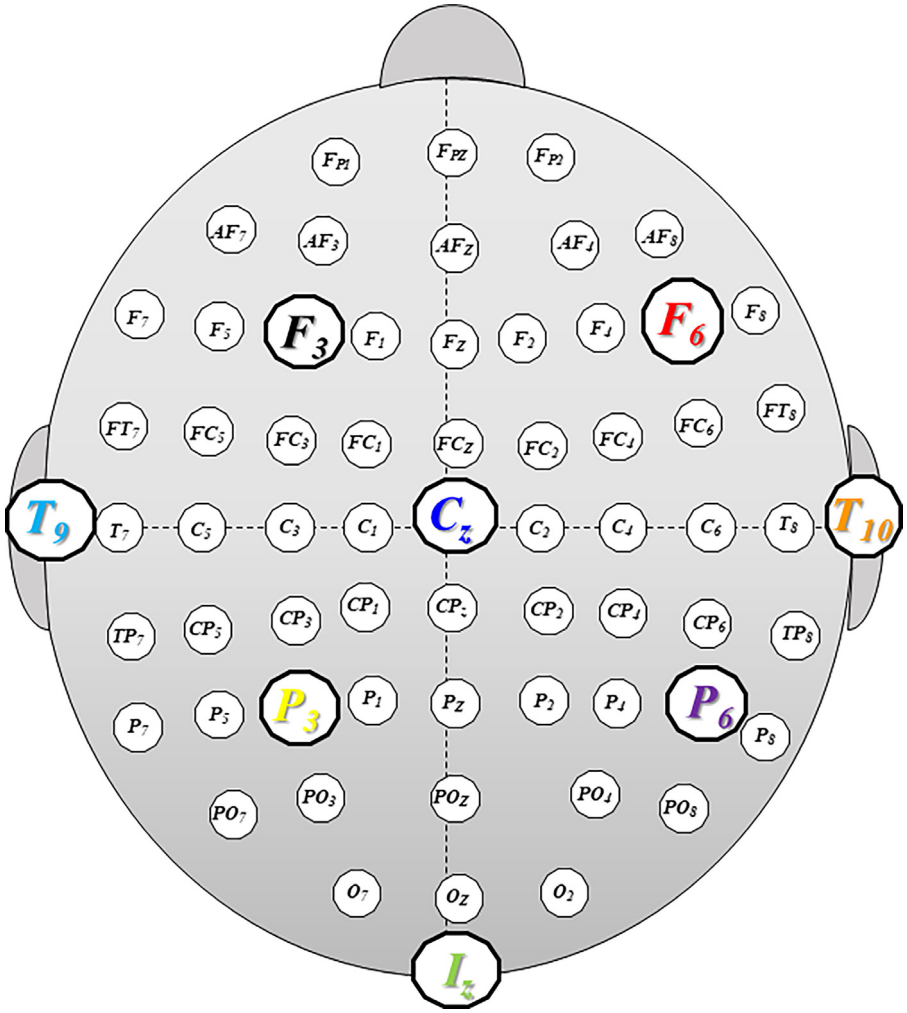

Fig. 1. International 10–10 system of 64 EEG electrodes. The highlighted broken lines circles identify the locations of the eight EEGs-channels used in this paper, i.e.: frontal F_3 and F_6; temporal T_9 and T_{10}; parietal P_3 and P_6; occipital I_z; and central C_z.

2. Experimental protocol and DFA statistical method

2.1. Experimental protocol

The experimental data used in this work were extracted from the well-known *Physionet* database, available at the address [29]:

https://archive.physionet.org/pn4/eegmmidb/

This dataset consists of over 1500 one and two-minute EEG recordings, obtained from 109 volunteers. From this set to analyze their EEG, we chose 11 subjects randomly, represented here by:

$$S_{010},\ S_{020},\ S_{029},\ S_{043},\ S_{046},\ S_{050},\ S_{051},\ S_{060},\ S_{071},\ S_{086},\ S_{099}$$

Each subject executed different real/imagery motor tasks. These tasks were initialized in answer to different events when the subject observed some targets. In real motor experiments, the target appears on either the left or the right side of the screen. The subject opens and closes the corresponding fist until the target disappears. Then the subject relaxes. At later time, the imagery motor tasks were executed, when the target appears on the same sides on the screen equal to the real motor tasks, the subject imagines opening and closing the corresponding fist until the target disappears. Then the subject relaxes. Within the experimental protocol, the chosen EEGs were measured when the volunteers performed the following real/imagery motor tasks:

Task 1 open and close left or right fists;

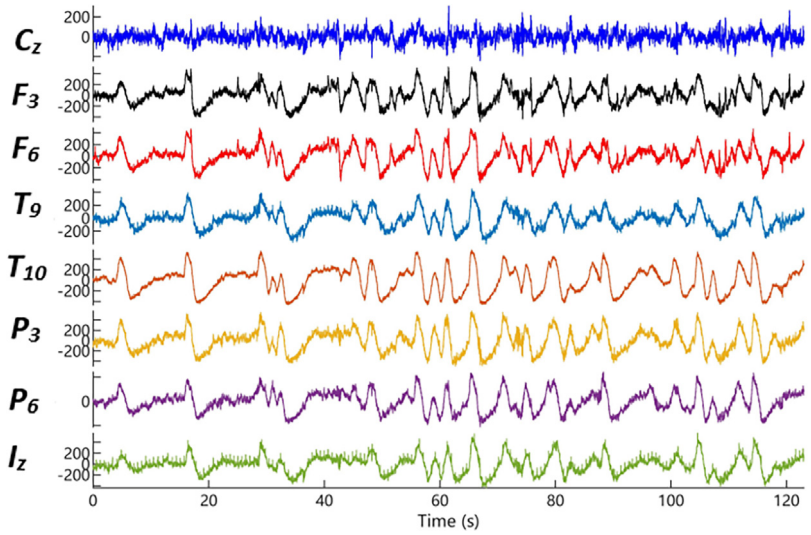

Fig. 2. EEG time series from subject S_{010} performing the **Task 1**, with the following channels: C_z, F_3, F_6, T_9, T_{10}, P_3, P_6 and I_z.

Task 2 imagine opening and closing left or right fists;

Task 3 open and close both fists or both feets;

Task 4 imagine opening and closing both fists or both feets.

The EEGs were measured using a 64-channel BCI2000 system [30]:
http://www.bci2000.org
with a sampled frequency of 160 samples per second and saved in EDF+ format. In Fig. 2, as an example for the EEG signals. We can observe the time series about eight channels from the subject S_{010} performing the **Task 1**.

2.2. DFA statistical method

Proposed by Peng [31], the DFA-based method proved to be a tool capable of providing a priori parameter to detect the auto-correlation of non-stationary temporal signals. The main advantage of the DFA method, in comparison with other fractal analysis methods, is to avoid spurious detection of unreal correlations, which are non-stationarity artifacts [32,33]. The steps to be follow for apply the DFA-based method, considering a signal $u(i)$ (such as an EEG bio-signal), where $i = 1, \ldots, N_{max}$, and N_{max} is the length of the EEG time series, were:

(1) Obtain the integrated time series by, $y(k) = \sum_{i=1}^{k}[u(i) - \langle u \rangle]$, here $\langle u \rangle$ represent the average value of $u(i)$;
(2) The integrated bio-signal $y(k)$ is decomposed into boxes of equal size n (time scale);
(3) For each n size box, we fit $y(k)$, using a polynomial function of order ≥ 1, called by $y_n(k)$.;
(4) The integrated signal $y(k)$ is detrended by subtracting the local trend $y_n(k)$ in each box of length n;
(5) The $F_{DFA}(n)$ root mean square fluctuation (rms) function for this integrated and detrended signal is compute by,

$$F_{DFA}(n) = \sqrt{\frac{1}{N_{max}} \sum_{k=1}^{N_{max}} [y(k) - y_n(k)]^2} \tag{1}$$

These steps are repeated fora all time scales between $4 \leq n \leq N_{max}/4$.

(6) Finally, we need to investigate if the relationship between $F_{DFA}(n)$ and the box size (n), behaves a power-law, according to Eq. (2) below,

$$F_{DFA}(n) \propto n^{\alpha_{DFA}} \tag{2}$$

In the affirmative case, then α_{DFA} exponent can be interpreted as a long-range correlation exponent, namely an auto-affinity parameter. This relation is normally illustrated in a $\log F(n) \times \log(n)$ graph, being represented by a straight line with slope equal to α_{DFA}. To know more about this coefficient, see the Table 1.

Following the methodology, the approach using the function $\Delta \log F_{DFA}$, have the proposal of measure the difference in the fluctuation amplitude between two EEGs channels [24,26]. This tool is an enhancement given to the DFA method [31], and has been shown to be useful when applied to the analysis of electrophysiological signals. Using this function, we can

Table 1
Statistical interpretation of the exponent α_{DFA}.

α_{DFA} exponent	Signal type
$\alpha_{DFA} < 0.5$	Anti-persistent
$\alpha_{DFA} \simeq 0.5$	Uncorrelated, white noise
$\alpha_{DFA} > 0.5$	Long-range correlated persistent
$\alpha_{DFA} \simeq 1$	$1/f$ noise
$\alpha_{DFA} > 1$	Non-stationary
$\alpha_{DFA} \simeq 3/2$	Brownian noise

study how much two brain regions are auto-correlated on the same scale (coherence temporal). In practice, we applied the DFA-based method on two temporal series and their logarithms individually are calculated by Eq. (3), taking as an example the F_3 and any other xx channel:

$$\Delta \log F_{DFA}[F_3 : xx] = \log F_{DFA}[F_3] - \log F_{DFA}[xx] \tag{3}$$

In this case we can have three possible conditions, these are:

(a) $\Delta \log F_{DFA}[F_3 : xx] > 0$: the amplitude of $F_{DFA}[F_3]$ function on channel F_3 is **larger** if compared with $F_{DFA_{xx}}$ from xx channel;
(b) $\Delta \log F_{DFA}[F_3 : xx] = 0$: the amplitude of $F_{DFA}[F_3]$ function on channel F_3 is **similar** with $F_{DFA_{xx}}$ from xx channel;
(c) $\Delta \log F_{DFA}[F_3 : xx] < 0$: the amplitude of $F_{DFA}[F_3]$ function on channel F_3 is **smaller** if compared with $F_{DFA_{xx}}$ from xx channel.

It is important to note that the DFA method itself performs only self-affinity analysis for only a single time series, as well as the $\Delta \log F_{DFA}$ function. With the intention of measuring cross-correlations between two time series, Podobnik [34] created the Detrended Cross-Correlation Analysis (DCCA) method, generalization of the DFA, to estimate the cross-correlation between two non-stationary time series by means of the detrended covariance function, F_{DCCA}. Therefore, repeating the similar procedure described in DFA method for two time series, it is possible to verify the existence or not of cross-correlation power-law, described by

$$F^2_{DCCA} \propto n^{2\lambda} \tag{4}$$

Here, λ describes the long-range cross-correlation exponent. The exponent λ identifies and measures long-range cross-correlations between two signals in different time scales n, but does not quantify the level of cross-correlation. To quantify this level of cross-correlation, Zebende [27] proposed the cross-correlation coefficient, ρ_{DCCA}. The DCCA cross-correlation coefficient is obtained as the ratio between the DCCA covariance function $F^2_{DCCA[X_i,Y_i]}(n)$, and each DFA auto-correlation function by:

$$\rho_{DCCA}(n) = \frac{F^2_{DCCA[X_i,Y_i]}(n)}{F_{DFA[X_i]}(n) F_{DFA[Yi]}(n)} \tag{5}$$

This DCCA cross-correlation coefficient is dimensionless and range between:

$$-1 \leq \rho_{DCCA} \leq 1.$$

In this case, if $\rho_{DCCA} = -1$, we have perfect anti cross-correlation. If $\rho_{DCCA} = 0$, then we have no cross-correlation. If, $\rho_{DCCA} = 1$, we will get a perfect cross-correlation between the time series $\{X_i\}$ and $\{Y_i\}$. Also, in [35,36] was reported that the DCCA cross-correlation coefficient dominates the Pearson coefficient for non-stationary series analysis.

3. Results and discussions

Initially with the time series of the EEG from 11 subjects, we calculated the F_{DFA} function, for each set of motor tasks (**Real/Imaginary**) in response to the **Right/Left** and **Top/Down** visual stimulus. To detail the influence of the F_{DFA} method, we calculated the traditional coefficient α_{DFA} for all possible time scale and for three different time scales (choice made visually and also with the best adjustments):

- all time scale: $4 \leq n \leq 4564$;
- time scale **I**: $n \leq 16$;
- time scale **II**: $16 < n \leq 723$;
- time scale **III**: $n > 723$.

Following Fig. 1, we used only 8 channels distributed over the brain: **frontal** F_3 and F_6; **temporal** C_z, T_9 and T_{10}; **parietal** P_3 and P_6; **occipital** I_z. Each time series containing 19.680 points with approximately 2 minutes, and a sampling period of the $\Delta T = 6.25$ ms. As an example, in Fig. 3 is shown the behavior of F_{DFA} as a function of n for all time scale and for the S_{010},

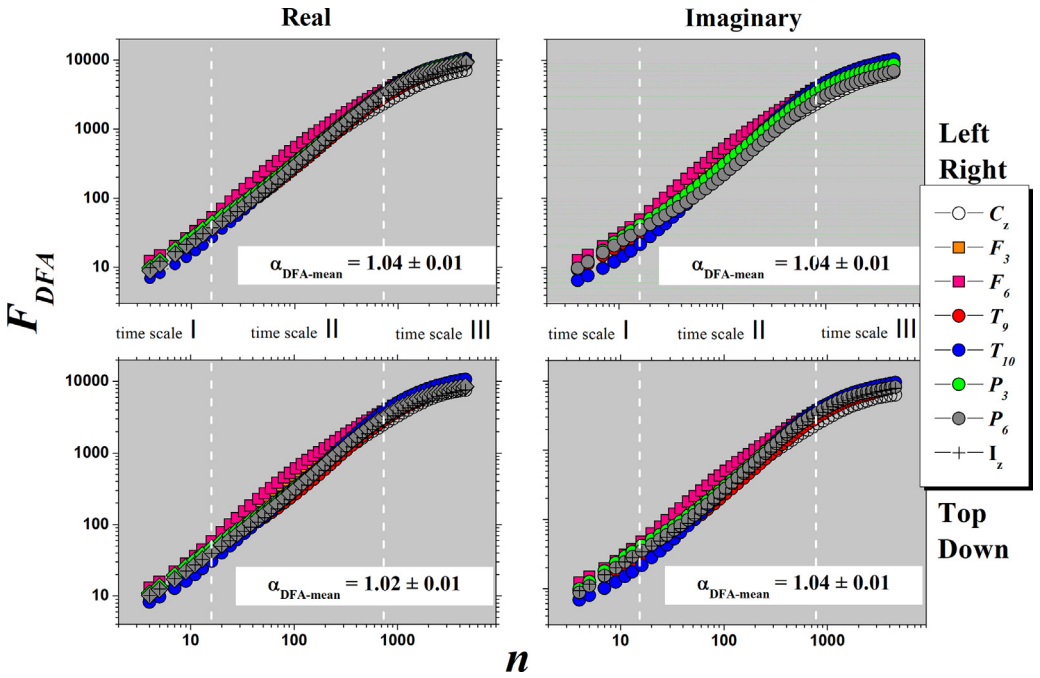

Fig. 3. F_{DFA} as a function of n for subject S_{010} performing all 4 Tasks. The continuous yellow line defines the linear fit of the experimental data for all time scale. The different auto-correlation exponents and the associated errors are also presented. Vertical dashed lines represent the time scale (**I**, **II**, **III**).

in this case performing all four tasks: Open/Close (Real/Imaginary) the Left/Right fists, and Open/Close (Real/Imaginary) both fists (Top) or both feet (Down), depending the visual stimulus on screen. The auto-correlation exponent α_{DFA} values for all tasks are greater than 1. These reveal that the EEGs are non-stationary series with long-range persistence or self affinity, in according with previous reports [35]. Interpreting Fig. 3 more deeply, we can state that the EEG signals in **Task 1** and **Task 2** are very similar, because:

$$\alpha_{DFA}(Real) = \alpha_{DFA}(Imaginary)$$

(Real) = (Imaginary) which means that **Task 1** and **Task 2** represent the same metal activity. The same conclusion can be made about the **Task 3** and **Task 4**, with α_{DFA}(Real) - α_{DFA}(Imaginary) of approximately 0.07. These preliminary results, with S_{010}, assertively shows that it is indifferent to carry out Real or Imaginary experiments to study brain motor activity.

For better accuracy, we now did it with a sample of 11 subjects and the eight channels. The results for α_{DFA} (in time scale **I**, **II** and **III**) can be seen in Table 2 . In this Table we present the mean value of α_{DFA} for the 11 subjects. The results for $\langle\alpha_{DFA}\rangle$ mean are presented in the Table 2, indicating a scale-dependent pattern.

Here we can see that in the overall average of the 11 subjects and all channels (last line in the Table 2), there are no major changes if the experiment was Real or Imaginary, because the auto-correlation exponent are very similar. Therefore, if we look at each channel separately, we can see that each one has its characteristic value of $\langle\alpha_{DFA}\rangle$ (higher values for the front channels). Also, we can observe for small ($n \leq 16$) and medium ($16 < n \leq 723$) time scale, $0.99 < \langle\alpha_{DFA}\rangle < 1.22$. For large time scales ($n > 723$), $\langle\alpha_{DFA}\rangle$ presents a value lower than 0.5, except for the channels C_z, F_3, F_6, and T_9, when executed the Real tasks, and the channel C_z, for the Imaginary task. Based on the Table 1, in general between the time scale **I** and time scale **II** we can observe the transition between non-stationary and noise signals, for Real/Imaginary experiments. Lastly, in the time scale **III**, $\langle\alpha_{DFA}\rangle < 0.5$, showing an anti-persistent behavior on this scale.

Now, knowing that the front channel F_3 has the greatest amplitude of fluctuation, revealed by [24], here was calculated the function $\Delta \log F_{DFA}[F_3 : xx]$ described in Eq. (3), in order to measure on average where there is greater relative brain activity and in which time scale. This result is presented in Fig. 4. This figure shows the relationship between two points of the brain. Generally, it is possible to observe a positive difference in the fluctuation amplitude for all time scales and channels, in other words,

$$\Delta \log F_{DFA}[F_3 : xx] \geq 0.$$

However, if we compare the channel F_3 with the channel F_6 (also on the front of the scalp), we can see that

$$\Delta \log F_{DFA}[F_3 : F_6] \simeq 0.$$

Table 2
Mean values of α_{DFA} for all experiments. The first column contains the stimuli (Left/Right or Top/Down), second column the channel, third (Real case), and fourth (Imaginary case) represent the α_{DFA} at time scale: **I** ($n \leq 16$), **II** ($16 < n \leq 723$) and **III** ($n > 723$).

Task	Channel	Real			Imaginary		
		I	**II**	**III**	**I**	**II**	**III**
Left/Right	C_z	1.10	0.94	0.57	1.07	0.93	0.50
	F_3	1.19	1.00	0.51	1.01	0.97	0.42
	F_6	1.21	0.94	0.51	1.19	0.89	0.38
	T_9	1.04	1.16	0.51	1.08	1.21	0.48
	T_{10}	1.14	1.14	0.44	1.18	1.21	0.39
	P_3	1.04	1.04	0.40	1.02	1.1	0.40
	P_6	1.08	1.11	0.41	0.93	1.23	0.48
	I_z	0.99	1.16	0.47	1.05	1.08	0.37
	Mean	1.10	1.06	0.48	1.07	1.08	0.43
Top/Down	C_z	1.09	0.95	0.39	1.05	0.96	0.39
	F_3	1.21	0.90	0.32	1.17	0.91	0.33
	F_6	1.22	0.88	0.39	1.18	0.90	0.36
	T_9	1.01	1.14	0.42	0.99	1.12	0.41
	T_{10}	1.15	1.18	0.38	1.20	1.02	0.35
	P_3	1.03	1.06	0.33	1.03	1.02	0.29
	P_6	1.06	1.10	0.35	1.05	1.09	0.30
	I_z	0.98	1.06	0.37	0.96	1.12	0.34
	Mean	1.09	1.03	0.37	1.08	1.02	0.35

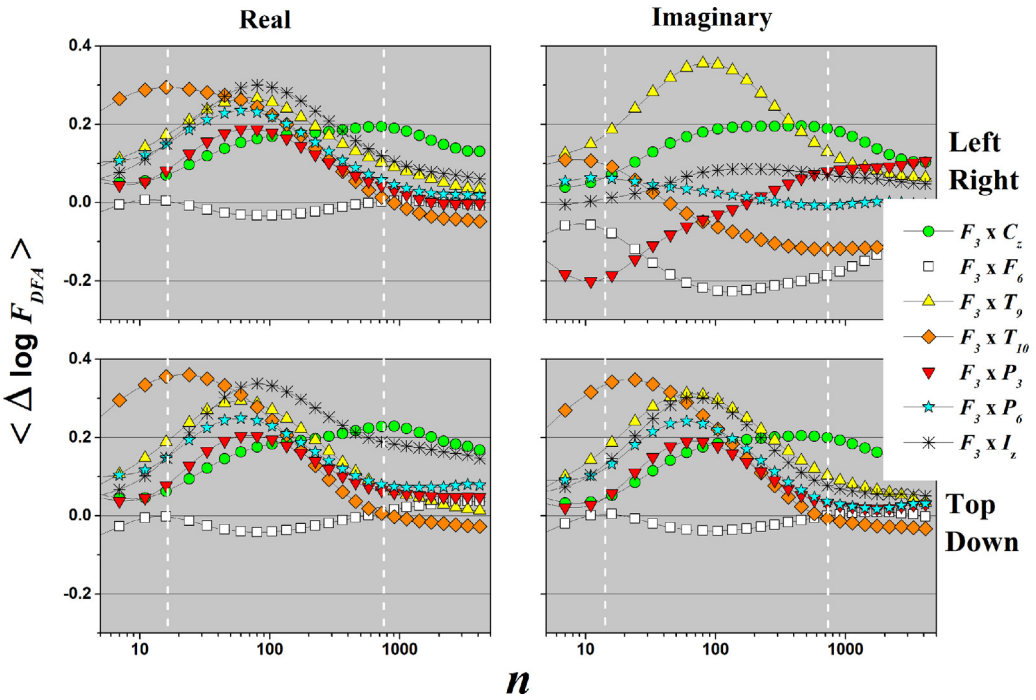

Fig. 4. Mean value of $\Delta \log F_{DFA}[F_3 : xx]$ as a function of n, considering the difference between the channel F_3 and the channels: C_z, F_6, T_9, T_{10}, P_3, P_6 and I_z. Vertical dashed lines represent the time scale (**I**, **II**, **III**).

This result evidences the greater activity in the frontal part of the brain. It is verified that for other channels, excepting F_6, that $\Delta \log F_{DFA}[F_3 : xx]$ has its maximum value. For large time scale, $n > 1000$, $\Delta \log F_{DFA}[F_3 : xx]$ tends to a constant value.

As the last case of study in relation to the tasks performed by the 11 subjects, and considering the level of adherence between the EEG channels, we will apply from this point the DCCA cross-correlation coefficient, ρ_{DCCA}, between the signals (7 channels) having as support the channel F_3. The results for this application are shown in Fig. 5, with $\langle \rho_{DCCA} \rangle$ mean. In Fig. 5, there is positive cross-correlation for all channels if compared to the channel F_3. The channels C_z, F_6, T_9, and T_{10}, are those that have a higher level of DCCA cross-correlation if compared to the channel F_3 (in this order), and the

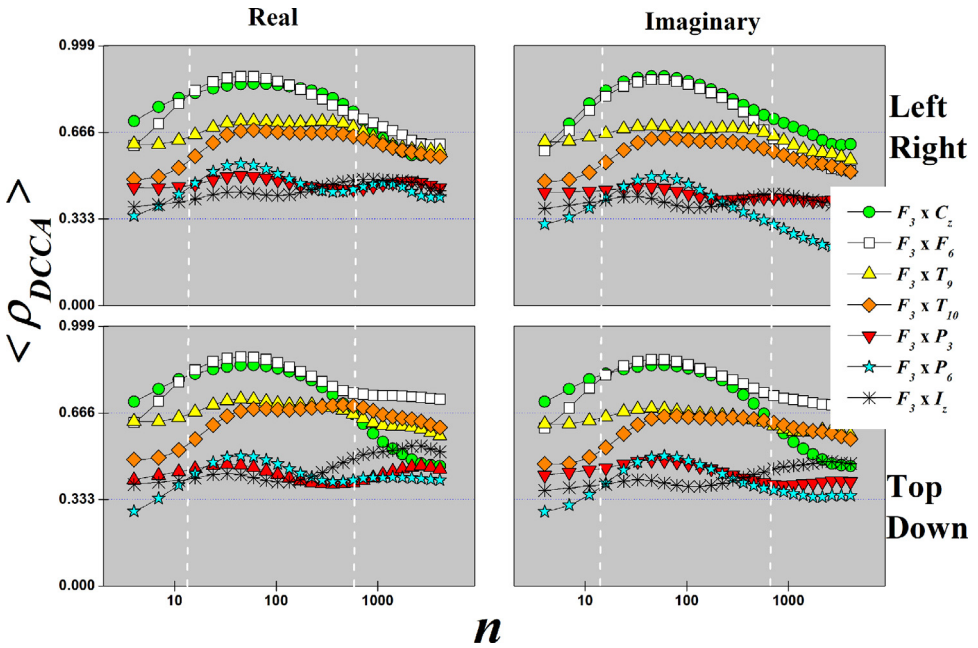

Fig. 5. Mean values for ρ_{DCCA} as a function of n. Each curve represent the cross correlation between the channel F_3 with the other channels, represented here by: C_z, F_6, T_9, T_{10}, P_3, P_6 and I_z. Vertical dashed lines represent the specific time scale (**I**, **II**, **III**).

time scale **II**, with $16 < n \leq 723$ is the time scale with ρ_{DCCA} maximum. It is possible to notice that the value of ρ_{DCCA} its similar for all talks, Real/Imaginary, Left/Right or Top/Down. This behavior presented by ρ_{DCCA} is probably due to the stimulus presentation time and consequently the brain response, when the subjects are performing the tasks

4. Conclusions

Through the statistical analysis of time series, it is proved that the proposed DFA based methods are capable of quantitatively describing similarities when the brain performs the same motor task in a real or imaginary way. Consequently, considering a referenced EEG database, we can assertively conclude that: The statistical results first showed us that there are three important time scales, which are, **I** ($n \leq 16$), **II** ($16 < n \leq 723$), and **III** ($n > 723$), as well as, from the point of view of DFA auto-correlation, α_{DFA}(Real) = α_{DFA}(Imaginary), for all time scales. Also, in order to compare the fluctuation amplitude of an EEG signal in relation to the other channels, we applied the $\Delta \log F_{DFA}$. Thus, choosing the F_3 channel (front) as the reference, we identified generally that, $\Delta \log F_{DFA}[F_3 : xx] \geq 0$ at its average value, except for the channel F_6 (also on the front of the scalp) that has a value for $\Delta \log F_{DFA}[F_3 : F_6] \simeq 0$. With DCCA cross-correlation coefficient, we can see that $\rho_{DCCA} > 0$, showing that the same brain signal/response was measured for all channels. The channels: C_z, F_6, T_9, and T_{10}, are those that have a higher level of DCCA cross-correlation, if compared to the channel F_3. The time scale **II**, with $16 < n \leq 723$, is the one with ρ_{DCCA} maximum. The ρ_{DCCA} statistic, quantify high temporal coherence similitude of the EEGs performed by the brain, between the Real and Imaginary motor human tasks. For this reason, is plausible choose the ρ_{DCCA} to quantitative study, this Real/Imaginary brain motor function, or possibly other types of the EEGs. Finally, the statistic applied in this paper, based on the DFA-method, proved to be an excellent candidate for studies of motor functions in the brain computer interface area.

CRediT authorship contribution statement

F.M. Oliveira Filho: Conceptualization, Methodology, Sofware, Writing – original draft, Visualization, Validation, Writing – review & editing. **F.F. Ribeiro:** Conceptualization, Visualization. **J.A. Leyva Cruz:** Conceptualization, Methodology, Sofware, Writing – original draft, Visualization, Validation, Writing – review & editing. **A.P. Nunes de Castro:** Sofware. **G.F. Zebende:** Conceptualization, Methodology, Software, Writing – original draft, Visualization, Validation, Writing – review & editing.

Declaration of competing interest

The authors declare the following financial interests/personal relationships which may be considered as potential competing interests: Gilney Figueira Zebende and Florêncio Mendes de Oliveira Filho reports financial support provided by National Council for Scientific and Technological Development.

Data availability

Data will be made available on request.

Acknowledgments

G. F. Zebende thanks the Brazilian agency CNPq (Conselho Nacional de Desenvolvimento Científico e Tecnológico), Brazil (Grant 310136/2020-2). F. M. Oliveira Filho thanks the Brazilian agency CNPq (Conselho Nacional de Desenvolvimento Científico e Tecnológico), Brazil (Grant 150655/2022-3). We would also like to thank Chico Mendes, rubber tapper, political activist and Brazilian environmentalist (*in memoriam*).

References

[1] K. Linkenkaer-Hansen, V.V. Nikouline, J.M. Palva, R.J. Ilmoniemi, Long-range temporal correlations and scaling behavior in human brain oscillations, J. Neurosci. 21 (4) (2001) 1370–1377.
[2] A. Biasiucci, B. Franceschiello, M.M. Murray, Electroencephalography, Curr. Biol. 29 (3) (2019) R80–R85.
[3] F.L. da Silva, EEG and MEG: relevance to neuroscience, Neuron 80 (5) (2013) 1112–1128.
[4] H. Berger, Über das elektroenkephalogramm des menschen, Archiv Für Psychiatrie Und Nervenkrankheiten 87 (1) (1929) 527–570.
[5] D. Cohen, Magnetoencephalography: detection of the brain's electrical activity with a superconducting magnetometer, Science 175 (4022) (1972) 664–666.
[6] M.C. Piastra, A. Nüßing, J. Vorwerk, M. Clerc, C. Engwer, C.H. Wolters, A comprehensive study on electroencephalography and magnetoencephalography sensitivity to cortical and subcortical sources, Human Brain Mapping 42 (4) (2021) 978–992.
[7] M. Ploner, E.S. May, Electroencephalography and magnetoencephalography in pain research—current state and future perspectives, Pain 159 (2) (2018) 206–211.
[8] S. Ibrahim, R. Djemal, A. Alsuwailem, Electroencephalography (EEG) signal processing for epilepsy and autism spectrum disorder diagnosis, Biocybern. Biomed. Eng. 38 (1) (2018) 16–26.
[9] Y. Höller, A.C. Bathke, A. Uhl, N. Strobl, A. Lang, J. Bergmann, R. Nardone, F. Rossini, H. Zauner, M. Kirschner, et al., Combining SPECT and quantitative EEG analysis for the automated differential diagnosis of disorders with amnestic symptoms, Front. Aging Neurosci. 9 (2017) 290.
[10] K. Batista García-Ramó, C.A. Sanchez Catasus, L. Morales Chacón, A. Aguila Ruiz, A. Sánchez Corneaux, P. Rojas López, J. Bosh Bayard, A novel noninvasive approach based on SPECT and EEG for the location of the epileptogenic zone in pharmacoresistant non-lesional epilepsy, Medicina 55 (8) (2019) 478.
[11] R. Esposito, M. Bortoletto, C. Miniussi, Integrating TMS, EEG, and MRI as an approach for studying brain connectivity, The Neuroscientist 26 (5–6) (2020) 471–486.
[12] H. Yu, J. Liu, L. Cai, J. Wang, Y. Cao, C. Hao, Functional brain networks in healthy subjects under acupuncture stimulation: An EEG study based on nonlinear synchronization likelihood analysis, Phys. A 468 (2017) 566–577.
[13] H. Yu, X. Wu, L. Cai, B. Deng, J. Wang, Modulation of spectral power and functional connectivity in human brain by acupuncture stimulation, IEEE Trans. Neural Syst. Rehabil. Eng. 26 (5) (2018) 977–986.
[14] H. Yu, X. Li, X. Lei, J. Wang, Modulation effect of acupuncture on functional brain networks and classification of its manipulation with EEG signals, IEEE Trans. Neural Syst. Rehabil. Eng. 27 (10) (2019) 1973–1984.
[15] H. Yu, X. Lei, Z. Song, C. Liu, J. Wang, Supervised network-based fuzzy learning of EEG signals for Alzheimer's disease identification, IEEE Trans. Fuzzy Syst. 28 (1) (2020) 60–71.
[16] D.G. de Figueiredo, Análise de Fourier E Equações Diferenciais Parciais, IMPA, Projeto Euclides, 1977.
[17] E. Kanasewich, The fast Fourier transform: Time sequence analysis in geophysics, third ed., The University of Alberta Press, 1974.
[18] R. Sedgewick, Algorithms in C, Princeton Universit, 1995, Cap.41 - The Fast Fourier Transform p.583.
[19] T. Montez, S.-S. Poil, B.F. Jones, I. Manshanden, J.P. Verbunt, B.W. van Dijk, A.B. Brussaard, A. van Ooyen, C.J. Stam, P. Scheltens, et al., Altered temporal correlations in parietal alpha and prefrontal theta oscillations in early-stage Alzheimer disease, Proc. Natl. Acad. Sci. 106 (5) (2009) 1614–1619.
[20] V.V. Nikulin, E.G. Jönsson, T. Brismar, Attenuation of long-range temporal correlations in the amplitude dynamics of alpha and beta neuronal oscillations in patients with schizophrenia, Neuroimage 61 (1) (2012) 162–169.
[21] S. Lahmiri, Generalized hurst exponent estimates differentiate EEG signals of healthy and epileptic patients, Phys. A 490 (2018) 378–385.
[22] H.-C. Chiu, H.-P. Ma, C. Lin, M.-T. Lo, L.-Y. Lin, C.-K. Wu, J.-Y. Chiang, J.-K. Lee, C.-S. Hung, T.-D.W. abd Li-Yu Daisy Liu, Y.-L. Ho, Y.-H. Lin, C.-K. Peng, Serial heart rhythm complexity changes in patients with anterior wall ST segment elevation myocardial infarction, Sci. Rep. 7 (2017) 43507.
[23] A. Pavlov, A. Runnova, V. Maksimenko, O. Pavlova, D. Grishina, A. Hramov, Detrended fluctuation analysis of EEG patterns associated with real and imaginary arm movements, Phys. A 509 (2018) 777–782.
[24] G.F. Zebende, F.M. Oliveira Filho, J.A. Leyva Cruz, Auto-correlation in the motor/imaginary human EEG signals: A vision about the FDFA fluctuations, PLoS ONE 12 (9) (2017) e0183121.
[25] V. Mesquita, F. Oliveira Filho, P.C. Rodrigues, Detection of crossover points in detrended fluctuation analysis: an application to EEG signals of patients with epilepsy, Bioinformatics 37 (9) (2021) 1278–1284.
[26] F. Oliveira Filho, J.L. Cruz, G. Zebende, Analysis of the EEG bio-signals during the reading task by DFA method, Phys. A 525 (2019) 664–671.
[27] G.F. Zebende, DCCA cross-correlation coefficient: Quantifying level of cross-correlation, Phys. A 390 (4) (2011) 614–618.
[28] Y. Chen, L. Cai, R. Wang, Z. Song, B. Deng, J. Wang, H. Yu, DCCA cross-correlation coefficients reveals the change of both synchronization and oscillation in EEG of Alzheimer disease patients, Phys. A 490 (2018) 171–184.
[29] A.L. Goldberger, L.A. Amaral, L. Glass, J.M. Hausdorff, P.C. Ivanov, R.G. Mark, J.E. Mietus, G.B. Moody, C.-K. Peng, H.E. Stanley, PhysioBank, PhysioToolkit, and PhysioNet: components of a new research resource for complex physiologic signals, Circulation 101 (23) (2000) e215–e220.
[30] G. Schalk, D.J. McFarland, T. Hinterberger, N. Birbaumer, J.R. Wolpaw, BCI2000: a general-purpose brain-computer interface (BCI) system, IEEE Trans. Biomed. Eng. 51 (6) (2004) 1034–1043.
[31] C.-K. Peng, S.V. Buldyrev, S. Havlin, F. Sciortino, H.E. Stanley, Long-range correlations in nucleotide sequences, Nature 356 (1992) 168–170.
[32] D. Mirzayof, Y. Ashkenazy, Preservation of long range temporal correlations under extreme random dilution, Phys. A 389 (24) (2010) 5573–5580.
[33] C. Heneghan, G. McDarby, Establishing the relation between detrended fluctuation analysis and power spectral density analysis for stochastic processes, Phys. Rev. E 62 (5) (2000) 6103.
[34] B. Podobnik, H.E. Stanley, Detrended Cross-Correlation Analysis: A new method for analyzing two nonstationary time series, Phys. Rev. Lett. 100 (8) (2008) 084102.
[35] D.A. Blythe, V.V. Nikulin, K.-R. Müller, Robust statistical detection of power-law cross-correlation, Sci. Rep. 6 (1) (2016) 1–10.
[36] L. Kristoufek, Measuring correlations between non-stationary series with DCCA coefficient, Phys. A 402 (2014) 291–298.